Holzforschung, Vol. 64, pp. 353–361, 2010 • Copyright © by Walter de Gruyter • Berlin • New York. DOI 10.1515/HF.2010.041

Mixed mode fracture testing of adhesively bonded wood specimens using a dual actuator load frame

Hitendra K. Singh[1,a], Abhijit Chakraborty[2,b], Charles E. Frazier[3] and David A. Dillard[1,*]

[1] Engineering Science and Mechanics Department, Virginia Tech, Blacksburg, VA, USA
[2] Mechanical Engineering, Virginia Tech, Blacksburg, VA, USA
[3] Wood Science and Forest Products Department, Virginia Tech, Blacksburg, VA, USA

*Corresponding author.
Engineering Science and Mechanics Department, Virginia Tech, Blacksburg, VA 24061, USA
Phone: +1-540-231-4714
E-mail: dillard@vt.edu
[a] Currently at Research & Technology Department, Cooper Tire & Rubber Company, 701 Lima Avenue, Findlay, OH 45840, USA.
[b] Currently at Aerospace and Engineering Mechanics Department, University of Minnesota, Minneapolis, MN 55455, USA.

Abstract

An experimental evaluation of mixed mode fracture tests conducted on adhesively bonded wood specimens using a dual actuator load frame is presented. This unit allows the fracture mode mixity to be easily varied during testing of a given specimen, providing improved consistency, accuracy, and ease of testing over a range of loading modes. Double cantilever beam (DCB) type specimens made of southern yellow pine (*Pinus* spp.) wood substrates bonded with a commercially available one part polyurethane adhesive were tested over a wide range of mode mixities from pure mode I to pure mode II. The critical strain energy release rate (SERR) values were calculated from the measured load, displacement, and crack length data, in combination with material properties and specimen geometric parameters, and compared on a $\mathcal{G}_{\mathrm{I}}$ versus $\mathcal{G}_{\mathrm{II}}$ fracture envelope plot. Mean quasi-static fracture energy values were calculated to be 390 J m^{-2} and 420 J m^{-2} for mode I and mode II fracture, respectively. For various mixed mode phase angles, the critical SERR values were partitioned into mode I and mode II components. In mixed mode loading conditions the cracks were typically driven along the interface, which resulted in lower total fracture energy values when compared with those measured under pure mode I loading conditions. A drop in measured fracture energy of approximately 45% was observed with mode mixity phase angles as small as 16°, implying that engineering designs based on results from the popular mode I DCB test could be nonconservative in some situations. Fracture surfaces obtained at different mode mixities are also discussed. An improved understanding of fracture behavior of adhesively bonded wood joints under mixed mode loading through generation of fracture envelopes could lead to improved designs of bonded wood structures.

Keywords: dual actuator load frame; fracture envelope; fracture mechanics; mixed mode I/II; mode I; mode II; strain energy release rate (SERR); wood adhesion.

Introduction

Adhesive bonding of wood components has played an essential role in the development and growth of the forest products industry (Chow 1983; Vick 1999) and has been a key factor in the efficient utilization of timber resources. However, the sometimes unpredictable and misunderstood behavior of wood-adhesive joints, including fracture, is a significant challenge to improving the performance of existing products and the development of new wood-based structures. The fracture of wood-adhesive joints often begins with the microscopic initiation of a crack at some flaw in the material or, in this case, the bonded joint. The initial flaw can be a discontinuity, such as a void, or an abrupt change in material properties. By nature, wood contains innumerable discontinuities, such as the cell cavity and transition zones between cell wall layers (Dinwoodie 1981). An adhesive can contain air bubbles or fillers with properties different from the resin. A rough wood surface might not be completely wetted by the adhesive, leaving voids at the interface. The adhesive and wood also have different mechanical properties contributing to stress concentrations (Williams 1952) in regions of material or geometric mismatch, such as in junctions where materials with different stiffnesses meet or wherever geometric discontinuities occur. Also, stresses resulting from differential shrinkage and swelling of the bonded members or wood fragments could add to these pre-existing stresses and contribute to the initiation of fracture and joint failure.

Fracture can occur in a pure mode or in some combination of the three fracture propagation modes: mode I (opening), mode II (forward shear), and mode III (tearing or out-of-plane) (Broek 1982). The in-plane modes, I and II, are usually believed to be most common or important and have been the subject of the majority of fracture tests and analyses. In homogeneous materials, cracks will tend to turn so that they grow perpendicular to the largest tensile stress (Erdogan and Sih 1963), growing in a mode I manner (Cotterell and Rice 1980). In non-homogeneous systems, such as adhesive joints, or anisotropic materials, such as wood, property variations tend to constrain crack growth, often forcing propagation under mixed mode conditions. To develop comprehensive failure envelopes spanning the full range of mode mixities, a number of pure and mixed mode tests must be conducted. These mixed mode conditions are quantified by a mode mixity phase angle, ψ, defined as (Hutchinson and Suo 1992):

$$\psi = \tan^{-1}\sqrt{\frac{\mathcal{G}_{II}}{\mathcal{G}_{I}}} \quad (1)$$

where $\psi = 0°$ refers to pure mode I and $\psi = 90°$ refers to pure mode II loading conditions. Several studies have been conducted to investigate the effect of mode mixity on fracture of adhesively bonded joints (Liechti and Hanson 1988; Liechti and Freda 1989; Liechti and Chai 1992; Liang and Liechti 1995; Swadener and Liechti 1998; Parvatareddy and Dillard 1999) and the path taken by growing cracks (Fleck et al. 1991; Chen and Dillard 2001a,b; Chen et al. 2001, 2002). Extensive research has been conducted to characterize the fracture properties of bonded wood specimens under mode I (Ebewele et al. 1980; Takatani et al. 1985; River et al. 1989; Scott et al. 1992; River and Okkonen 1993) and mode II (Barrett 1981; Fonselius 1992; Frühmann et al. 2002) configurations, but little testing (Wu 1967; Mall et al. 1983; Valentin and Caumes 1989) has been done to explore the effect of mixed mode loading, which typically requires specialized specimen geometries and/or fixtures (Jernkvist 2001; Mansfield-Williams 2001).

This study utilizes a newly developed dual actuator load frame to perform mixed mode testing on bonded beam specimens consisting of wood adherends. With support from the National Science Foundation (NSF), we have developed a unique research instrument capable of providing an instantaneously and infinitely variable mode mixity for fracture mechanics studies of adhesively bonded beam specimens, laminated composites, and other beam-like specimens. A schematic of the dual actuator instrument is presented in Figure 1. A personal computer and controller (not shown in Figure 1) direct both actuator control and automated data acquisition. The pump is a standard hydraulic pump used on servo-hydraulic test systems. The design allows one to produce any desired combination of in-plane mode mixity with a single standard specimen, such as that used for the double cantilever beam (DCB) specimen advocated by ASTM D-3433-99 (2001). The flexibility in applied mode mixity is achieved through the use of two actuators driven by standard servo-controllers, which can be independently operated at any desired amplitude and phase difference. Each actuator is equipped with a load cell and displacement sensor to provide information necessary for quantitative evaluation of specimen behavior. The specimen is clamped at the lower end, and loads are applied to the debonded end through appropriate clevises attached to the adherends. The advantages of this device include the following:

1. Mode mixity is infinitely variable from pure mode I to pure mode II. (Extension to mode III testing is possible as well through the use of scarfed bond planes.)
2. Mode mixity can be changed instantaneously by varying the amplitude of the loading actuators, allowing rapid variations of mode mixity to address important scientific questions concerning the effect on locus of failure and fracture energy.
3. Data at various mode mixities can be obtained with a single specimen or specimen type, providing increased consistency, accuracy, and convenience in determining mode mixity effects.
4. The unit is capable of conducting quasi-static and fatigue tests on specimens held in a controlled temperature chamber, or submersed in a liquid environment, as permitted by a horizontal axis machine.
5. The unit offers the potential to systematically characterize fracture envelopes for adhesively bonded systems, to address scientific questions related to fracture propagation under complex loading, and to develop technological insights for improving the performance and design of such materials.

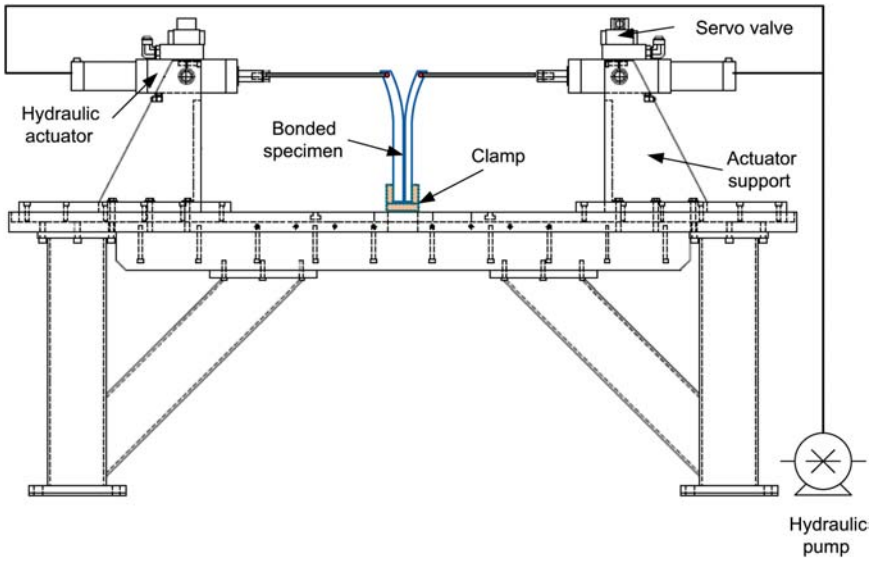

Figure 1 Schematic illustration of the dual actuator load frame.

More details on the instrument design and other aspects can be found elsewhere (Dillard et al. 2006, 2010; Singh et al. 2006).

Experimental

Specimen preparation

DCB specimens were made by bonding two wood substrates (southern yellow pine, *Pinus* spp.) with Gorilla Glue® (The Gorilla Glue Company, Cincinnati, OH, USA), a one-part moisture-cure polyurethane adhesive purchased from a local vendor. The southern yellow pine (*Pinus* spp.) lumber used was flat sawn to 50 mm thick and obtained locally. This lumber was machined into 145 mm × 230 mm × 11 mm thick laminae with a longitudinal grain angle of approximately 3–5°, as described by Gagliano and Frazier (2001) and shown in Figure 2a–c. Grain angle control strongly promotes crack propagation within the bond rather than into the substrate. All wood laminae were then conditioned at 20 ± 1°C and 65 ± 1% relative humidity (RH) in an environmental chamber for approximately 2 weeks until they attained 12% equilibrium moisture content (EMC). This step was taken to minimize any differential swelling in these laboratory specimens for testing purposes, fully recognizing that bonded wooden joints exposed to general service environments can experience additional debonding energies because of residual stresses present (Guo et al. 2006). Immediately prior to adhesive application, bonding surfaces were planed to provide a final thickness of 10 mm. The adhesive was only applied to the bonding surface of one of the laminae by using a hard rubber roller maintaining an approximate adhesive coverage of 156 g m^{-2}. The bonding surface of the other laminae was moistened with water using a wet paper towel without precise control. The laminae were then consolidated into a laminate at room temperature under a pressure of 0.87 MPa (126 psi) for 24 h. The edges of the bonded laminate were removed prior to cutting the laminate into four or five 20 mm wide fracture specimens.

A mode I pre-cracking process was incorporated for all bonded specimens to develop a sharp crack tip prior to the initial loading procedure. To aid in pre-cracking the specimens, a 25-mm long initial debond area was created by using a colored paraffin-based marker at the loading end of the bonded DCB specimen. The other end of the bonded specimen was clamped in a table-top vise. For all specimens tested in mode I manner, a C-clamp was placed at a point that was approximately 55 mm from the load application point for all specimens to facilitate crack arrest during the pre-cracking procedure. To ensure specimen stability, a C-clamp was placed at a point that was approximately 60% of the total specimen free length for all mixed mode and mode II specimens for this same purpose (Hashemi et al. 1990; Kinloch et al. 1993; Choi et al. 1999; Simón et al. 2005). A stainless-steel wedge was then lightly hammered into the bonded joint region, allowing the wood adherends to separate

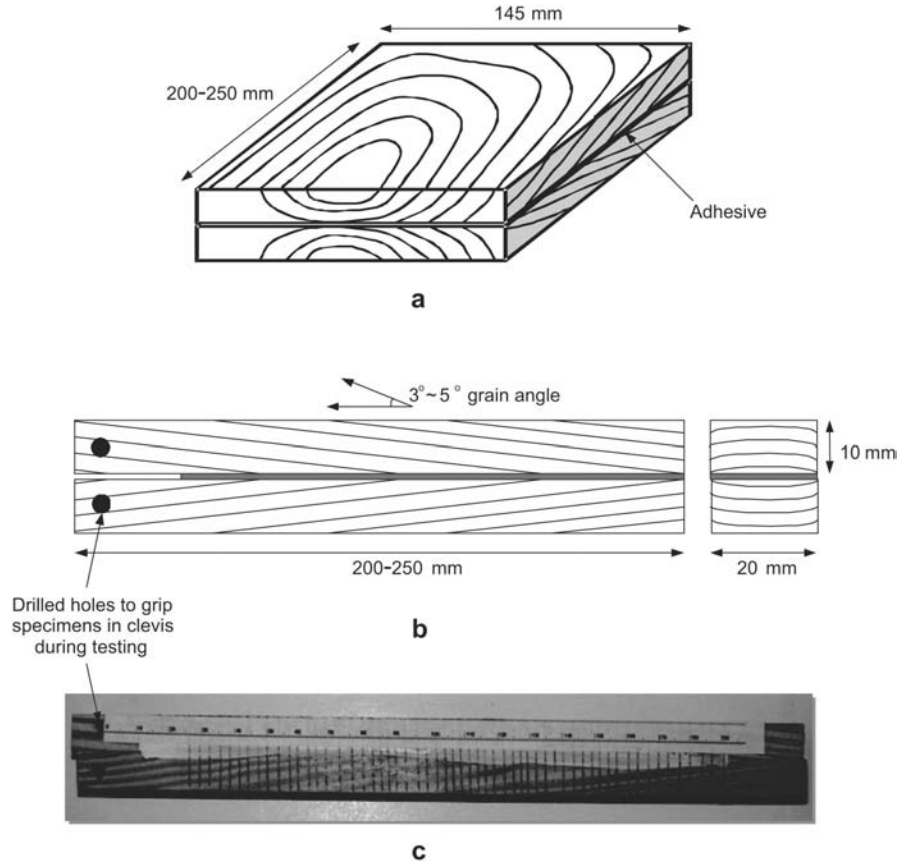

Figure 2 Double cantilever beam (DCB) sample preparation method: (a) two wooden laminates bonded together with polyurethane adhesive, (b) illustration of a typical DCB specimen with dimensions and grain angle obtained from cutting the bonded wood laminate into 4 or 5 specimens, (c) DCB sample painted with white correction fluid and marked with parallel lines along with the attached paper scale.

up to the clamped region of the specimen, thus developing a sharp crack tip suitable for testing. Each individual bonded specimen was then drilled with 3 mm diameter holes using a drilling template produced specifically for this purpose. These holes allow for mounting the two arms of the DCB specimens into clevises for testing. The use of a drilling template provided an accurate and repeatable drilling procedure to be used for each of the bonded specimens. For all tests, one side of each bonded specimen was painted white using water-based typewriter correction fluid, providing a brittle high-contrast coating that aids in crack detection. A series of parallel marks were drawn on this white region with a fine-point pen to provide a visual reference for measurement. A paper ruler with millimeter divisions was later attached to each specimen below the bondline to aid in visual crack length measurements during static tests. Typical bonded wood specimens are illustrated in Figure 2c.

Test procedure

All tests were conducted using the dual actuator load frame outfitted with a pair of 10 kN strain gage-based load cells and operated under displacement control mode. Load and displacement data were acquired by a host computer through a data acquisition (DAQ) card (PCI-6229, National Instruments Inc.) using custom designed National Instruments LabVIEW® (Austin, TX, USA) software. Each actuator is equipped with an extension arm attached to a clevis that mounts to the specimen ends using pins through the holes drilled in the adherends, as shown in Figure 2b,c. Prior to loading, the lower end of the fracture specimen was gripped in a bench vice fitted onto the bed of the dual actuator load frame, effectively clamping the bonded end of the specimen as required for asymmetric loading. During testing, the two debonded arms of the DCB beam were pinned in the clevises and loading was initiated by moving each actuator with a displacement rate chosen to provide the desired mode mixity. According to the procedure outlined by the European Structural Integrity Society (ESIS TC4) (Blackman and Kinloch 1997) (also reported in British standard BSI and BS-7991 2001), for crack length measurements, crack lengths were observed visually in relation to the attached paper rulers, as previously mentioned, and entered manually for the corresponding load and displacement using the LabVIEW® application. Using measured load, displacement, and crack length data, in combination with known material properties and specimen geometric parameters, mode I and mode II components of the applied strain energy release rate (SERR), $\mathcal{G}_{\mathrm{I}}$ and $\mathcal{G}_{\mathrm{II}}$, could be calculated for all configurations.

Data analysis

Many linear elastic fracture mechanics (LEFM) test configurations of bonded or laminated beam specimens involve applications of lateral loads or moments (Williams 1989a,b; Hashemi et al. 1990; Reeder and Crews 1992). Suo and Hutchinson (1990) derived a general analysis for the delamination shown in Figure 3a. A reviewer pointed out that Suo and Hutchinson (1990) omitted a coupling term that had been included in the experiments of Davidson and Schapery (1990) and Williams (1988), but this did not lead to an error as no axial forces were involved in our tests. The specimen is a bonded beam specimen loaded with arbitrary bending moments at the crack tip. The expression for the total SERR, given in Eq. (2) (Hutchinson and Suo 1992), can be written in terms of the applied moments, M_1 and M_2, applied in the wake of the crack tip to the right and left adherends, respectively, and the uncracked portion bending moment M_1-M_2 as follows:

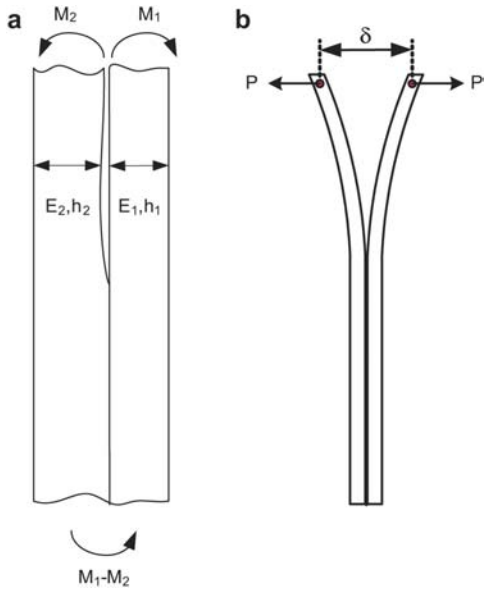

Figure 3 Double cantilever beam (DCB) specimen (a) loaded with arbitrary bending moments and (b) loaded under mode I configuration.

$$\mathcal{G} = \frac{1}{2B}\left[\frac{M_1^{\,2}}{E_1 I_1} + \frac{M_2^{\,2}}{E_2 I_2} - \frac{(M_1 - M_2)^2}{E_2 B q h_1^{\,3}}\right] \tag{2}$$

where subscripts 1 and 2 represent the right and left adherends, h_1 and h_2 are the thicknesses of the right and left adherends, E is the elastic modulus, I represents the second moment of area of the adherends, B is the width of the adherends and bond, and q is given as:

$$q = \Sigma\left[\left(\Lambda - \frac{1}{\eta}\right)^2 - \left(\Lambda - \frac{1}{\eta}\right) + \frac{1}{3}\right] + \frac{\Lambda}{\eta}\left[\Lambda - \frac{1}{\eta}\right] + \frac{1}{3\eta^3}$$

where, $\Lambda = \dfrac{1 + 2\Sigma\eta + \Sigma\eta^2}{2\eta\eta\,(+\Sigma\eta)}$, $\Sigma = \dfrac{E_1}{E_2}$ and $\eta = \dfrac{h_1}{h_2}$. For $h_1 = h_2 = h$ and $E_1 = E_2$, Eq. (2) can be partitioned into mode I and mode II components as follows (Williams 1988):

$$\mathcal{G}_{\mathrm{I}} = \frac{3(M_1 + M_2)^2}{B^2 E h^3} \tag{3}$$

$$\mathcal{G}_{\mathrm{II}} = \frac{9(M_1 - M_2)^2}{4B^2 E h^3} \tag{4}$$

By varying the ratio of the two applied moments, the full mode mixity range from pure mode I to pure mode II can be generated. To take into account the effects of beam shear, crack tip deflection and beam root rotation, Eqs. (3) and (4) can be written in a modified form (Williams 1989a,b; Blackman et al. 1991) as:

$$\mathcal{G}_{\mathrm{I}} = \frac{(P_1 + P_2)^2 (a + \Delta_{\mathrm{I}})^2}{4B(EI)_{\mathrm{eff}}} \tag{5}$$

$$\mathcal{G}_{\mathrm{II}} = \frac{3(P_1 - P_2)^2 (a + \Delta_{\mathrm{II}})^2}{16B(EI)_{\mathrm{eff}}} \tag{6}$$

where the mode II crack length correction factor, Δ_{II}, is approximated as 0.42 Δ_I, where Δ_I is the mode I crack length correction factor determined from a standard DCB test (Wang and Williams 1992). Effective flexural rigidity $(EI)_{eff}$ and Δ_I are determined from the experimental data by the following relationships:

$$(EI)_{eff} = \frac{2}{3m^3} \tag{7}$$

$$\Delta_I = \frac{b}{m} \tag{8}$$

where *m* and *b* are the slope and the *y*-intercept, respectively, from the linear trendline of the plot of the cube root of compliance versus crack length. Eqs. (5) and (6) derived above consider the effects of both shear deflection and root rotation (Williams 1989a,b). Examples of this method of data analysis can be found in the literature (Rakestraw et al. 1995; Gagliano and Frazier 2001).

Results and discussion

Three specimens were tested for each mode mixity phase angle and each specimen yielded approximately 6–10 data points for fracture energy calculations. To calculate an average value of the mode I crack length correction factor, Δ_I, three DCB specimens were tested in mode I configuration. For each fracture specimen, the compliance $\left(\frac{\delta}{P}\right)$ was calculated, where δ is the total displacement resulting from the applied load *P*, as shown in Figure 3b, and a straight line is fitted to the cube root of compliance plotted versus crack length, as shown in Figure 4. From this linear fit, the average values of slope *m* and intercept *b* were obtained and the values of $(EI)_{eff}$, Δ_I and Δ_{II} were calculated for this system. The value of the mode I critical SERR, $\mathcal{G}_{I_c}$, calculated using Eq. (5), is 390 ± 67 J m^{-2}, where the second number represents 1 SD. For the other mode mixity phase angles, three specimens each were tested and the values of $\mathcal{G}_I$ and $\mathcal{G}_{II}$ were calculated using Eqs. (5) and (6). Figure 5 shows the relationship between the components of the mixed mode SERR, $\mathcal{G}_I$ and $\mathcal{G}_{II}$, and the mode mixity phase angle, ψ. It should be noted that the connecting lines between the data points in Figure 5 are included only to guide the reader's eye for individual tests. It should also be noted that only one data point per specimen corresponding to a 90° phase angle (mode II configuration) was obtained; following this initiation, the crack propagated outside of the adhesive layer into the wood adherend. The value of mode II critical SERR, $\mathcal{G}_{II_c}$, calculated using Eq. (5), is 420 ± 62 J m^{-2}, which represents the initiation value while the crack tip is still apparently at the adhesive layer.

As shown in Figure 5, the mode I component of the critical strain energy release rate monotonically decreased with increasing ψ, whereas the mode II component gradually increased as ψ approached 90°. An increase of the mode II component with increasing mode mixity phase angle is generally found when the crack is located at an interface (Akisanya and Fleck 1992; Ikeda et al. 1998; Ducept et al. 2000) and can be attributed to factors such as the roughness of the crack surfaces, the presence of residual stresses, crack tip shielding, and the mismatch of elastic properties at the interface (Duer et al. 1996). To understand the role that stress plays in determining the mode of failure, note that in homogeneous isotropic materials, cracks propagate perpendicular to the direction of maximum tensile stress. In an adhesive joint subjected to a shear state, cracks within the adhesive layer have a tendency to grow toward one interface. Shear-dominated loading often results in interfacial failures or failures with less adhesive left on an interface (Chen and Dillard 2001a,b; Chen et al. 2001, 2002), although more complex hackle pattern failures have also been reported (Chai 1986).

Figure 6 shows the fracture envelope generated over the range of mode mixity phase angle. The scatter in the fracture energy data at each phase angle might be typical of natural

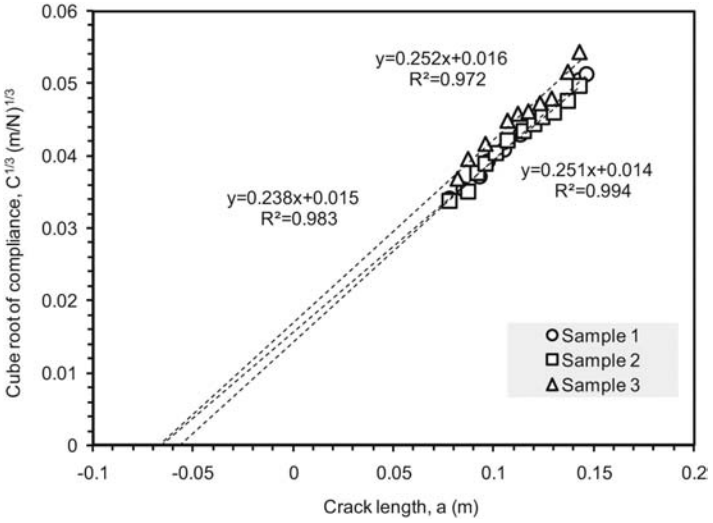

Figure 4 Cube root of compliance versus crack length for wood specimens tested under mode I configurations.

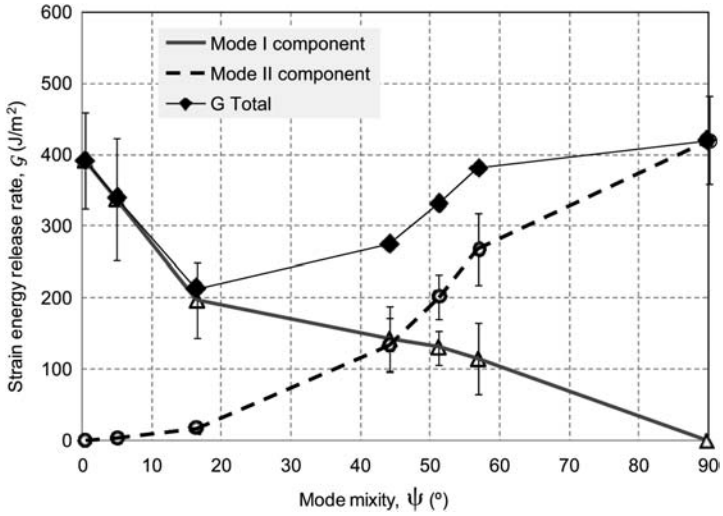

Figure 5 Variation of total value of strain energy release rate as well as mode I and mode II components as a function of mode mixity. Error bars indicate ±1 SD.

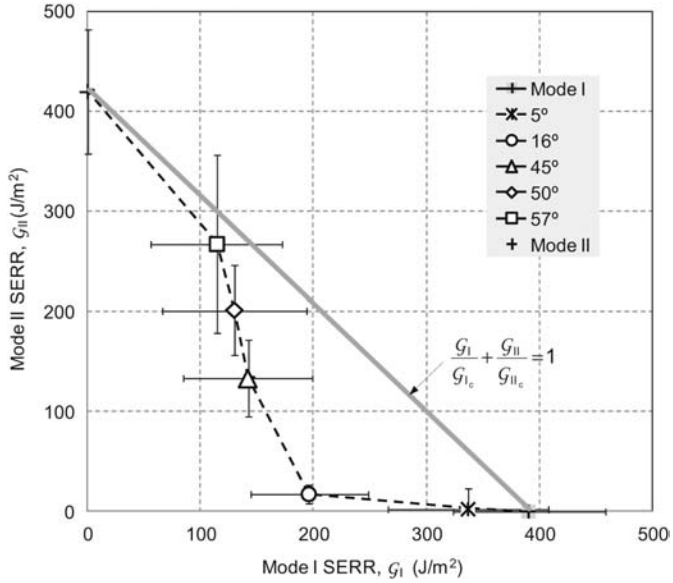

Figure 6 Mixed mode fracture envelope of southern yellow pine (*Pinus* spp.) bonded with polyurethane adhesive. Error bars indicate ±1 SD.

materials such as wood (Lim et al. 1994; Lim and Mizumachi 1995, 1997; Gagliano and Frazier 2001) and is partially attributed to the complex local stress patterns arising from a combination of grain periodicity (Mijovic and Koutsky 1979) and growth ring curvature and resulting variability in the bonding. Southern pines, used in this study as the adherend material, exhibit an abrupt transition between seasonal growth zones, respectively referred to as earlywood and latewood, corresponding to the period within the annual growth season. The material characteristics near adhesive bondline not only differ from specimen to specimen with regard to the periodicity of the growth rings, but also differ significantly within a single specimen. These factors ultimately contribute a great deal of variation in the data.

Aside from the scatter, the fracture envelope does suggest that the mode II fracture energy $\mathcal{G}_{II_c}$ is perhaps slightly higher than $\mathcal{G}_{I_c}$. If total fracture energy, $\mathcal{G}_c$, is a constant independent of mode mixity, one can write a fracture criteria (Broek 1982, 1988):

$$\frac{\mathcal{G}_I + \mathcal{G}_{II}}{\mathcal{G}_c} = 1 \tag{9}$$

Or where the critical fracture energies differ in mode I and II, an analogous criterion is (Broek 1982, 1988):

$$\frac{\mathcal{G}_{\mathrm{I}}}{\mathcal{G}_{\mathrm{I}_c}} + \frac{\mathcal{G}_{\mathrm{II}}}{\mathcal{G}_{\mathrm{II}_c}} = 1 \quad (10)$$

A gray line is shown in Figure 6 to convey this latter relationship. Of particular note is the abrupt drop in the total fracture energy as small amounts of mode II loading are applied, i.e., the total value of fracture energy, does not remain constant as mode mixity changes. This observation is clearly seen in Figure 5, where a drop in total fracture energy of approximately 45% was observed for a mode mixity of 16°. This is an important point to consider because designing adhesively bonded wood structures using only the mode I and mode II critical SERRs could be nonconservative. To simplify design, using the lowest fracture energy within the anticipated range of applied mode mixities might be appropriate.

After the fracture toughness tests, the fracture surfaces were examined optically to gain insight into the fracture mechanism and identify the fracture characteristics. A visual inspection of the failure surfaces revealed a relationship between mode mixity and the degree of fiber pullout and/or wood failure. Under pure mode I loading, the failure remained in the bondline with minor instances of shallow ($<$0.25–0.5 mm), earlywood fiber pullout. At a 5° mode mixity phase angle, the failure was similar to pure mode I, but the incidence of shallow, earlywood fiber pullout was more prevalent. At a 16° phase angle, the incidence of this fiber pullout seemed to decline from that observed at $\psi = 5°$. Although the relationship between fiber pullout and phase angle was not explicitly quantified, we noted that fiber pullout appeared less prevalent at $\psi = 16°$, corresponding to the dramatic reduction in total energy shown in Figure 5. At mode mixities of 45°, 50°, and 60°, failures were mostly confined to earlywood zones, but the fiber pullout was significantly deeper ($\sim$1–2 mm). In pure mode II loading, earlywood fiber pullout was considerably deeper (2–3 mm) and/or the substrate completely failed. In all cases it was noted that specimen grain angle control caused the crack to return to the adhesive layer, except when under pure mode II loading where complete substrate failure was observed in 2 out of 3 specimens tested.

Conclusions

The fracture behavior of southern yellow pine adherends bonded with a polyurethane adhesive was studied utilizing a newly developed dual actuator load frame. This instrument has significantly simplified the mixed mode testing of adhesively bonded wood joints, allowing a range of mode mixities to be evaluated with a common specimen and single test configuration. This instrument is a significant improvement over certain conventional techniques that are often time consuming to set up, cumbersome to use, and limited to a single mode mixity. Mixed mode fracture tests such as those performed in this study could provide significant insights into the fracture behavior of adhesively bonded wood structures.

In the case of southern yellow pine studied here, it was observed that the application of a small amount of mode II loading in the joint reduced the total fracture energy by 45%, a value significantly lower than that observed for either pure mode I or mode II conditions. This suggests that the introduction of a small amount of shear could reduce the total fracture energy of joints in some material systems. By measuring fracture energies of bonded specimens over a range of mixed mode loading conditions and generating fracture envelope, conservative estimates could be provided while designing wood structures subjected to mixed mode loading conditions.

The dual actuator load frame has proven to be very useful for characterizing fracture behavior over the entire range of mode I and II loading, providing a convenient method to characterize adhesion. The mixed mode fracture test results presented above, coupled with an appropriate mixed mode fracture criterion, should enable prediction of the fracture energy over the entire range of mode mixities. In doing so, models can be developed to help provide significant insight into understanding the fracture behavior of adhesively bonded structures. The examination of fracture surfaces revealed that with an increase in mode II loading component, the fracture of the wood adherends is increasingly adhesive resulting in an increasing amount of fiber pull-out and the crack growth pattern strongly depends on the global state of loading.

Acknowledgements

The material presented here is based upon the work supported by the National Science Foundation under contract DMR-0415840. We are grateful to the Engineering Science and Mechanics Department and Wood Science and Forest Products Department for the laboratory facilities. Special thanks go to Tian Gao, a graduate student in the Department of Wood Science and Forest at Virginia Tech, for supplying specimens and providing information on materials and specimen preparation and to Edoardo Nicoli for helpful comments. Finally, we are grateful to the reviewers for their constructive input.

References

Akisanya, A.R., Fleck, N.A. (1992) Brittle-fracture of adhesive joints. Int. J. Fract. 58:93–114.

ASTM D-3433-99 (2001) Standard test method for fracture strength in cleavage of adhesives in bonded metal joints. In: Annual Book of ASTM Standards. ASTM, West Conshohocken, PA. 15.06:225–231.

Barrett, J.D. (1981). Fracture mechanics and the design of wood structures. Philos. Trans. R. Soc. Lond. A Math. Phys. Sci. 299: 217–226.

Blackman, B.R.K., Kinloch, A.J. (1997) Determination of the mode I adhesive fracture energy, GIC, of structural adhesives using the double cantilever beam (DCB) and the tapered double cantilever beam (TDCB) specimens. E.S.I.S. (ESIS). ESIS TC4:38.

Blackman, B., Dear, J.P., Kinloch, A.J., Osiyemi, S. (1991) The calculation of adhesive fracture energies from double-cantilever beam test specimens. J. Mater. Sci. Lett. 10:253–256.

Broek, D. Elementary Engineering Fracture Mechanics. Sijthoff & Noordhoff, Alphen aan den Rijn, 1982.

Broek, D. Practical Use of Fracture Mechanics. Kluwer Academic Publisher, Dordrecht, 1988.

BSI and BS-7991 (2001) Determination of the mode I adhesive fracture energy, GIc, of structural adhesives using the double cantilever beam (DCB) and tapered double cantilever beam (TDCB) specimens.

Chai, H. (1986) A note on crack trajectory in an elastic strip bounded by rigid substrates. Int. J. Fract. 32:211–213.

Chen, B., Dillard, D.A. (2001a) The effect of the T-stress on crack path selection in adhesively bonded joints. Int. J. Adhes. Adhesives 21:357–368.

Chen, B., Dillard, D.A. (2001b) Numerical analysis of directionally unstable crack propagation in adhesively bonded joints. Int. J. Solids Struct. 38:6907–6924.

Chen, B., Dillard, D.A., Dillard, J.G., Clark, R.L. (2001) Crack path selection in adhesively-bonded joints: the role of material properties. J. Adhes. 75:405–434.

Chen, B., Dillard, D.A., Dillard, J.G., Clark, R.L. (2002) Crack path selection in adhesively bonded joints: the roles of external loads and specimen geometry. Int. J. Fract. 114:167–190.

Choi, N.S., Kinloch, A.J., Williams, J.G. (1999) Delamination fracture of multidirectional carbon-fiber/epoxy composites under mode I, mode II and mixed-mode I/II loading. J. Compos. Mater. 33:73–100.

Chow, S. (1983) Adhesive developments in forest products. Wood Sci. Technol. 17:1–11.

Cotterell, B., Rice, J.R. (1980) Slightly curved or kinked cracks. Int. J. Fract. 16:155–169.

Davidson, B.D., Schapery, R.A. (1990) A technique for predicting mode-I energy-release rates using a 1st-order shear deformable plate-theory. Eng. Fract. Mech. 36:157–165.

Dillard, D.A., Singh, H.K., Chakraborty, A., Park, S., Ohanehi, D. (2006) Mixed-mode fracture test results from a novel dual-actuator load frame. In: Proceedings of the 2006 SEM Annual Conference on Experimental Mechanics, Society for Experimental Mechanics, Inc., Bethel, CT. CD-ROM-Paper No. 10, June 4–7.

Dillard, D.A., Singh, H.K., Park, S., Ohanehi, D. (2010) A dual-actuator load frame for mixed-mode fracture of laminated or adhesively bonded specimens. Exp. Mech. in preparation.

Dinwoodie, J.M. Timber – Its Nature and Behavior. Van Nostrand Reinhold Company, New York, 1981.

Ducept, F., Davies, P., Gamby, D. (2000) Mixed mode failure criteria for a glass/epoxy composite and an adhesively bonded composite/composite joint. Int. J. Adhes. Adhesives 20:233–244.

Duer, R., Katevatis, D., Kinloch, A.J., Williams, J.G. (1996) Comments on mixed-mode fracture in adhesive joints. Int. J. Fract. 75:157–162.

Ebewele, R.O., River, B.H., Koutsky, J.A. (1980) Tapered double cantilever beam fracture tests of phenolic-wood adhesive joints. 2. Effects of surface-roughness, the nature of surface-roughness, and surface aging on joint fracture energy. Wood Fiber 12: 40–65.

Erdogan, V.F., Sih, G.C. (1963) On crack extension in plates under plane loading and transverse shear. Trans. ASME J. Bas. Eng. 85:519–527.

Fleck, N.A., Hutchinson, J.W., Suo, Z.G. (1991) Crack path selection in a brittle adhesive layer. Int. J. Solids Struct. 27:1683–1703.

Fonselius, M. (1992) Determination of fracture toughness for wood. J. Struct. Eng. 118:1727–1740.

Frühmann, K., Reiterer, A., Tschegg, E.K., Stanzl-tschegg, S.S. (2002) Fracture characteristics of wood under mode I, mode II and mode III loading. Philos. Mag. A 82:3289–3298.

Gagliano, J.M., Frazier, C.E. (2001) Improvements in the fracture cleavage testing of adhesively-bonded wood. Wood Fiber Sci. 33:377–385.

Guo, S., Dillard, D.A., Nairn, J.A. (2006) Effect of residual stress on the energy release rate of wedge and DCB test specimens. Int. J. Adhes. Adhesives 26:285–294.

Hashemi, S., Kinloch, A.J., Williams, J.G. (1990) The analysis of interlaminar fracture in uniaxial fiber-polymer composites. Proc. R. Soc. Lond. A Math. Phys. Eng. Sci. 427:173–199.

Hutchinson, J.W., Suo, Z. (1992) Mixed-mode cracking in layered materials. Adv. Appl. Mech. 29:63–191.

Ikeda, T., Miyazaki, N., Soda, T. (1998) Mixed mode fracture criterion of interface crack between dissimilar materials. Eng. Fract. Mech. 59:725–735.

Jernkvist, L.O. (2001) Fracture of wood under mixed mode loading II. Experimental investigation of *Picea abies*. Eng. Fract. Mech. 68:565–576.

Kinloch, A.J., Wang, Y., Williams, J.G., Yayla, P. (1993) The mixed-mode delamination of fiber composite-materials. Compos. Sci. Technol. 47:225–237.

Liang, Y.M., Liechti, K.M. (1995) Toughening mechanisms in mixed-mode interfacial fracture. Int. J. Solids Struct. 32:957–978.

Liechti, K.M., Hanson, E.C. (1988) Nonlinear effects in mixed-mode interfacial delaminations. Int. J. Fract. 36:199–217.

Liechti, K.M., Freda, T. (1989) On the use of laminated beams for the determination of pure and mixed-mode fracture properties of structural adhesives. J. Adhes. 28:145–169.

Liechti, K.M., Chai, Y.S. (1992) Asymmetric shielding in interfacial fracture under inplane shear. J. Appl. Mech. Trans. ASME 59: 295–304.

Lim, W.W., Mizumachi, H. (1995) Fracture-toughness of adhesive joints. 2. Temperature and rate dependencies of mode-I fracture-toughness and adhesive tensile-strength. J. Appl. Polym. Sci. 57:55–61.

Lim, W.W., Mizumachi, H. (1997) Fracture toughness of adhesive joints. 3. Temperature and rate dependencies of mode II fracture toughness and adhesive shear strength. J. Appl. Polym. Sci. 63: 835–841.

Lim, W.W., Hatano, Y., Mizumachi, H. (1994) Fracture-toughness of adhesive joints. 1. Relationship between strain-energy release rates in 3 different fracture modes and adhesive strengths. J. Appl. Polym. Sci. 52:967–973.

Mall, S., Murphy, J.F., Shottafer, J.E. (1983) Criterion for mixed-mode fracture in wood. J. Eng. Mech. ASCE 109:680–690.

Mansfield-Williams, H.D. (2001) An end-notched beam test for specific fracture energy in mixed mode in timber. Mater. Struct. 34:224–227.

Mijovic, J.S., Koutsky, J.A. (1979) Effect of wood grain angle on fracture properties and fracture morphology of wood-epoxy joints. Wood Sci. 11:164–168.

Parvatareddy, H., Dillard, D.A. (1999) Effect of mode-mixity on the fracture toughness of Ti-6Al-4V/FM-5 adhesive joints. Int. J. Fract. 96:215–228.

Rakestraw, M.D., Taylor, M.W., Dillard, D.A., Chang, T. (1995) Time dependent crack growth and loading rate effects on interfacial and cohesive fracture of adhesive joints. J. Adhes. 55: 123–149.

Reeder, J.R., Crews, J.H. (1992) Redesign of the mixed-mode bending delamination test to reduce nonlinear effects. J. Compos. Technol. Res. 14:12–19.

River, B.H., Okkonen, E.A. (1993) Contoured wood double cantilever beam specimen for adhesive joint fracture tests. J. Test. Eval. 21:21–28.

River, B.H., Scott, C.T., Koutsky, J.A. (1989) Adhesive joint fracture-behavior during setting and aging. Forest Prod. J. 39:23–28.

Scott, C.T., River, B.H., Koutsky, J.A. (1992) Fracture testing wood adhesives with composite cantilever beams. J. Test. Eval. 20: 259–264.

Simón, J.C., Johnson, E., Dillard, D.A. (2005) Characterizing dynamic fracture behavior of adhesive joints under quasi-static and impact loading. J. ASTM Int. 2:53–71.

Singh, H.K., Park, S., Ohanehi, D., Dillard, D.A. (2006) A design space for a novel dual-actuator mixed-mode test frame. In: Proceedings of the 29th Annual Adhesion Society Meeting, ed. Gregory Anderson, The Adhesion Society, Inc., Blacksburg, VA, pp. 157–159, February 19–22.

Suo, Z.G., Hutchinson, J.W. (1990) Interface crack between two elastic layers. Int. J. Fract. 43:1–18.

Swadener, J.G., Liechti, K.M. (1998) Asymmetric shielding mechanisms in the mixed-mode fracture of a glass/epoxy interface. J. Appl. Mech. Trans. ASME 65:25–29.

Takatani, M., Hamada, R., Sasaki, H. (1985) Cleavage fracture of wood epoxy-resin bond specimens in long-term loading. 2. Opening displacement and fracture-toughness. Mokuzai Gakkaishi 31:746–751.

Valentin, G., Caumes, P. (1989) Crack propagation in mixed mode in wood: a new specimen. Wood Sci. Technol. 23:43–53.

Vick, C.B. (1999) Adhesive bonding of wood materials. In: Wood Handbook: Wood as an Engineering Material. USDA Forest Service, Forest Products Laboratory, Madison, WI. pp. 9.1–9.24.

Wang, Y., Williams, J.G. (1992) Corrections for mode-II fracture-toughness specimens of composites materials. Compos. Sci. Technol. 43:251–256.

Williams, M.L. (1952) Stress singularities resulting from various boundary conditions in angular corners of plates in extension. J. Appl. Mech. 19:526–528.

Williams, J.G. (1988) On the calculation of energy-release rates for cracked laminates. Int. J. Fract. 36:101–119.

Williams, J.G. (1989a) End corrections for orthotropic DCB specimens. In: Composites Science and Technology, Elsevier Science Ltd, Kidlington, OX. 35:367–376.

Williams, J.G. (1989b) Fracture Mechanics of Anisotropic Materials, Application of Fracture Mechanics to Composite Materials. In: Ed., K. Friedrick, Composite Materials Series, Elsevier Science Publishers BV, Amsterdam. 6:3–38.

Wu, E.M. (1967) Application of fracture mechanics to anisotropic plates. J. Appl. Mech. 34:967–974.

Received May 3, 2008. Accepted November 11, 2009.
Previously published online February 17, 2010.